Pergamon

PII: S0191-8141(96)00081-8

Journal of Structural Geology, Vol. 19, No. 2, pp. 185 to 193, 1997

0191-8141/97 $17.00 + 0.00

Late-stage evolution of fault-propagation folds: principles and example

ERIC MERCIER, FATIMA OUTTANI and DOMINIQUE FRIZON DE LAMOTTE

Université de Cergy-Pontoise, Département des Sciences de la Terre (URA-CNRS 1369, groupe de Cergy-Pontoise), Le Campus, Av. du Parc, 95011 Cergy-Pontoise, Cedex, France

(*Received* 22 *November* 1995; *accepted in revised form* 23 *September* 1996)

Abstract—Fault-propagation folding commonly occurs near the fronts of mountain belts. This type of folding may even represent, in some thrust systems, the major mode of deformation. However, fault propagation folds are frequently altered by two kinds of late-stage evolution: breakthrough thrusting or transport on the flat. We model the geometric features of these kinds of fold, in particular the late stage modification, and present the algorithms and equations used in an original program. An application, based on an example from the Atlas mountains of Algeria, illustrates the main features of the model. © 1997 Elsevier Science Ltd. All rights reserved

INTRODUCTION

The main kinematic feature of a fault-propagation fold (FPF) is that folding and faulting occur synchronously. At each stage, during fault propagation, slip is completely accommodated by folding with no transfer of slip out of the fold, and it is zero at the ramp tip. The fold develops immediately above the ramp, which remains blind (Thompson, 1981). This geometry is usually clearly different from that of a fault-bend fold (Fig. 1). The fault-propagation fold model is put forward as an explanation for the common association of asymmetric folds with steep or overturned forelimbs adjacent to thrust faults.

Suppe and Medwedeff (1984) and Suppe (1985) established the geometric characteristics of fault-propagation folding. Subsequently, some typical structures of this type have been identified in fold-and-thrust belts (Jamison, 1987; Mitra and Namson, 1989; Mitra, 1990; Suppe and Medwedeff, 1990; Alonso and Teixell, 1992; Mitra, 1992), and it has now been demonstrated that in some thrust systems, fault-propagation folding represents the major mode of deformation (Mercier, 1992; Philippe, 1994; Outtani *et al.*, 1995; Martin and Mercier, 1996). However, in these areas, many natural folds with steeply-dipping forelimbs, exhibit later faulting that commonly breaks through the fold and obscures the original shape. It appears that the initial ideal geometry of FPF can be altered by a late-stage evolution, including hangingwall transport, that prevents an immediate identification (Suppe and Medwedeff, 1990; Mercier, 1992; Mercier *et al.*, 1994, 1995).

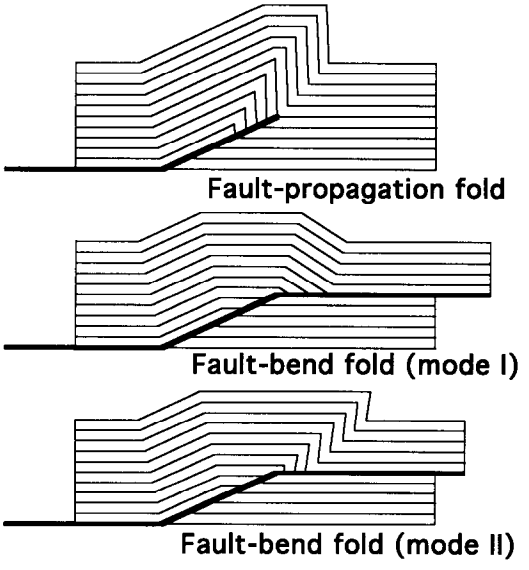

Fig. 1. The three main types of fold-thrust interactions (Suppe, 1983, 1985).

At any instant, fold growth may stop and subsequent fault propagation may cut through the fold itself. Following Jamison (1987), Suppe and Medwedeff (1990) and Mercier (1992), we will consider two families of sites for the development of breakthrough faults (Fig. 2). The first possible sites are located along the ramp. From these sites, 'steep-limb breakthrough thrusts' (Suppe and Medwedeff, 1990; Creuzot *et al.*, 1993) are developed, cutting through the forelimb of the previously built fold-propagation fold. The second possible sites are situated along inter-bed planes branching from the ramp tip. In this case, the slip on the new flat fault segment produces a 'transported FPF' resulting from transport on the flat of the previous FPF (Jamison, 1987; Mercier, 1992; McClay, 1992). This type of evolution corresponds to the 'décollement breakthrough structure' defined by Suppe and Medwedeff (1990).

This paper develops original quantitative models for the late stage evolution of FPF. The fundamental equations used to compute the shapes of the resulting structures are developed below. The main geological implications of this model are discussed based on a cross-section from the Atlas Mountains of Algeria.

PRINCIPLES OF MODELLING

The model proposed is a forward kinematic model. It consists of calculating the change in geometry resulting from the transport on the new fault.

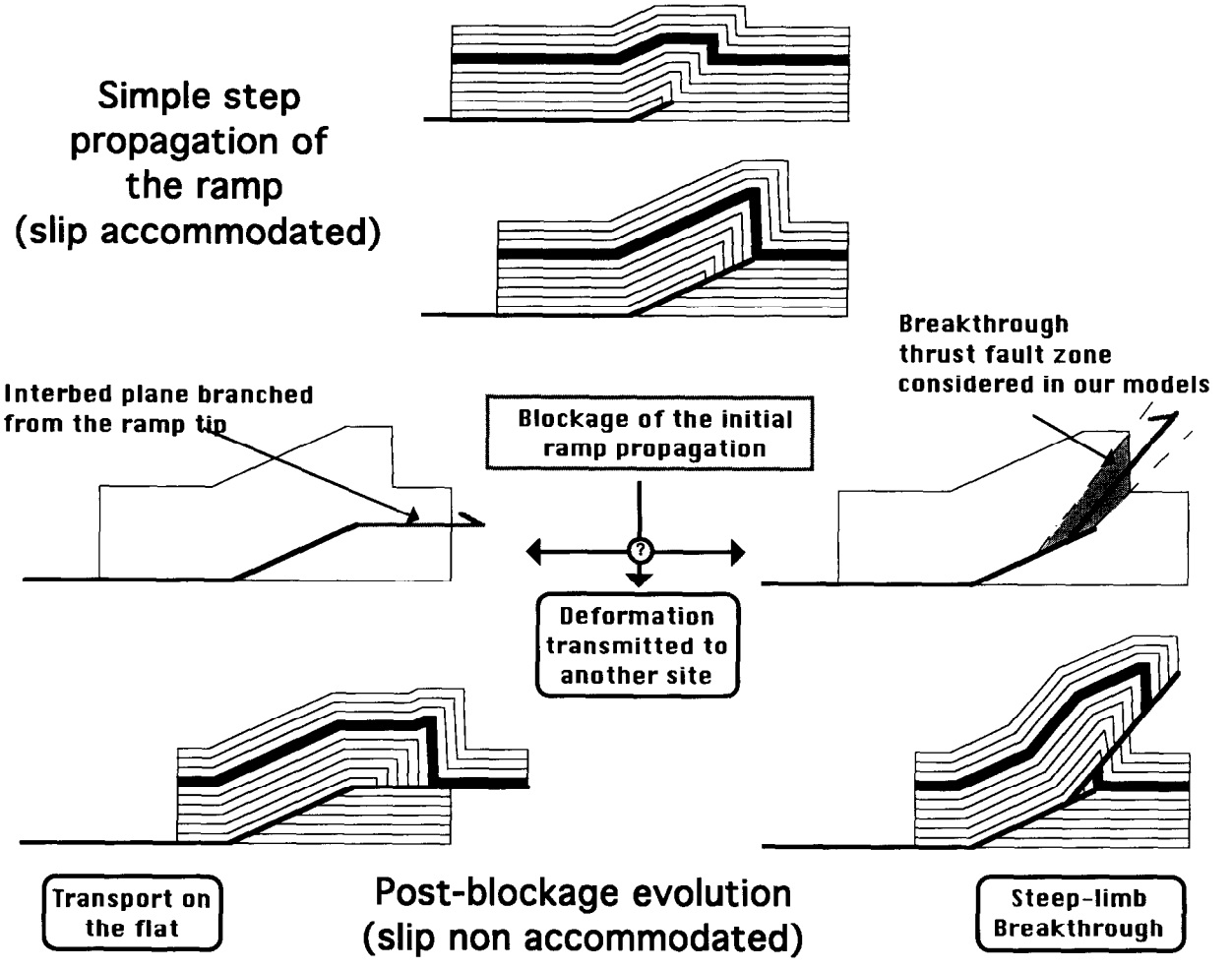

Fig. 2. Simple-step fault-propagation fold and the two kinds of late-stage modification. These were developed using the procedures described in this paper.

Geometry of a simple-step fault-propagation fold

Classically, it is assumed that area is preserved in the plane of the cross-section parallel to the transport direction. This hypothesis reduces the principle of mass and volume conservation to a two-dimensional problem. If it is also assumed that the thickness of beds is preserved between initial and final deformed states, the axial surface (kink-plane) bisects the angle between the two limbs of each hinge. In this case, the modelling of a FPF requires determination of the kink plane location (Suppe, 1983; Jamison, 1987). For this purpose, we must compute, for each kink, the dip of the axial plane and the precise location of one point on it. Finally, we need to know (Fig. 3):

(a) The location of the point B (ramp base); its coordinates (xB and yB) are input parameters in our models. (Note that here, and in all ensuing models, xP and yP are the horizontal and vertical coordinates of any point P.)

(b) The other input parameter is the value of the ramp angle (α). Angles γ and δ (see Fig. 3) depend on α; from Suppe (1985) these angles are related according to:

$$\delta = \gamma + \alpha, \tag{1}$$

$$1/\tan(\alpha) + 2\tan(\alpha/2) = 2/\tan(\gamma/2) - 1/\tan(\gamma). \tag{2}$$

No trivial solutions are available for the second equation. However, if the trigonometric identity:

$$\tan(x) = 2\tan(x/2)/(1 - \tan^2(x)/2) \tag{3}$$

recast in terms of α and γ, is substituted into equation (2) and rearranged, we find two possible solutions for γ:

$$\gamma = \pi - \alpha, \tag{4a}$$

$$\gamma = 2\arctan\left(3\tan\frac{\alpha}{2}\right). \tag{4b}$$

By combining equations (1) and (4a) we obtain

$$\delta = (\pi - \alpha) + \alpha = \pi.$$

The first solution (eq. 4a) is the pre-folding equation and the second (eq. 4b) is typically the post-folding equation. Figure 4 shows curves relating α and γ according to the second solution.

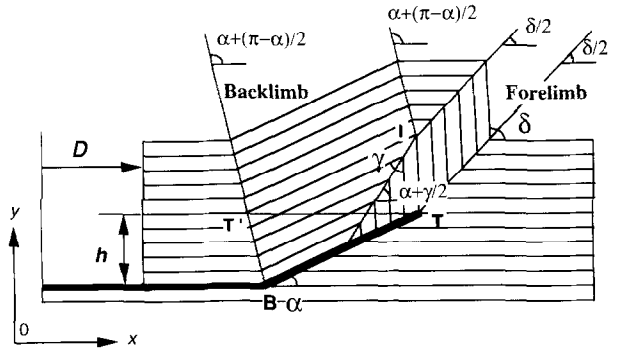

B = location of ramp base (xB,yB)
T = location of ramp top (xT,yY)
I = bifurcation point of anticlines hinges (xI,yI)
T' = projection of point T on the hinge of the back syncline (xT',yT')
D = accommodated displacement
h = ramp height
α = ramp angle
γ = interlimb angle
δ = forelimb characteristic dip angle

Fig. 3. Model of fault-propagation fold showing the parameters used in equations (1) to (9).

(c) The coordinates of the points T (ramp top), and I (bifurcation point of the anticlinal hinges) (Fig. 3) are related as:

$$xT = xB + \frac{h}{\tan(\alpha)}, \tag{5a}$$

$$yT = yB + h, \tag{5b}$$

$$xI = xT + \left(h \cdot \frac{\cos(\delta)}{\sin(\gamma)}\right), \tag{6a}$$

$$yI = yT + \left(h \cdot \frac{\cos(\delta)}{\sin(\gamma)}\right). \tag{6b}$$

Where h is the ramp height. Note that point I is on the same stratigraphic horizon as point T.

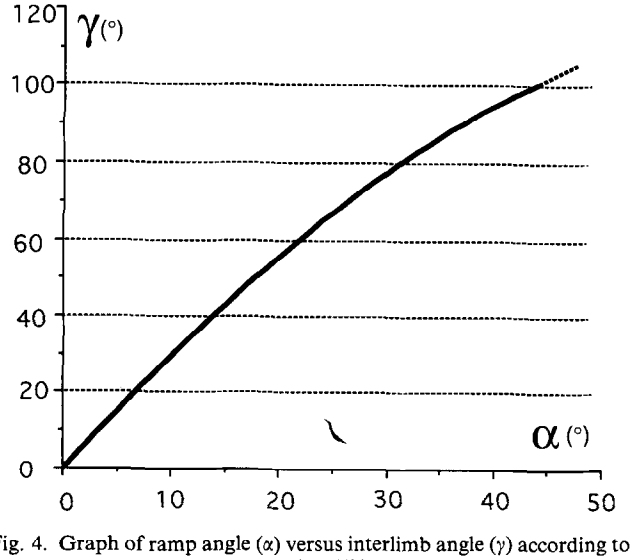

Fig. 4. Graph of ramp angle (α) versus interlimb angle (γ) according to equation (4b).

For balancing purposes it is important to know the value of displacement accommodated by the fold (D). It is equal to:

$$D = [TI] + [IT'] - [TT'], \tag{7}$$

where:

$$xT' = xB - h/\tan\left(\frac{\pi - \alpha}{2}\right), \tag{8a}$$

$$yT' = yB + h. \tag{8b}$$

From (7), (8a) and (8b), we have:

$$D = h\left[\frac{1 + \cos(\gamma)}{\sin(\gamma)} - \frac{1 - \cos(\alpha)}{\sin(\alpha)}\right]. \tag{9}$$

The above equations permit us to model each kink-plane for the fold. In this model, the planes bisect the angle between the two limbs of each fold. So, it is easy to draw any inter-bed if its original stratigraphic elevation above the lower décollement is known. Very simple geometric analysis permits locating the post-folding intersections of the inter-beds and the kink-planes. Note that if the inter-bed is stratigraphically above the ramp top, it is continuous from hangingwall to footwall. For beds situated below the ramp top, truncation by the ramp is predicted (Fig. 3).

Fault-propagation fold transported on the flat

Transport on the flat occurs when the fault reaches and follows a new décollement level rather than continuing to propagate through the fold. The slip generated along the upper flat is totally transferred to the front of the structure; a new input parameter is consequently introduced in the model: the value of 'non-accommodated' slip (D^*). During subsequent slip in the foreland direction, a new upper ramp hinge is formed. The part of the fold that was already located in front of the new active hinge (kink X) forms a 'residual' fold (Jamison, 1987) that undergoes a rigid-body translation (Figs 2 & 5). The backlimb that is transported through this active anticlinal hinge undergoes a bending parallel to the fault. But the problem is more complex for the portion of the forelimb which is initially located behind the hinge X (grey area in Fig. 5). These beds have an initial angle of cut-off against the ramp ($\pi - \gamma$) of $> 50°$ and must be transported through an anticlinal hinge which is related to a change in fault dip (α) of generally $> 10°$. Suppe (1983, fig. 7) showed that a parallel folding (constant thickness folding) solution does not exist for such a geometric situation. In other words, the beds of the forelimb portion transported through this anticline hinge must undergo non-parallel folding and a geometric alteration. Following Jamison (1987) and Mercier (1992), we assume that the axial plane of the kink fixed at the top of the ramp (kink X) bisects the angle between the ramp and the inter-bed activated as a slip-plane. As a

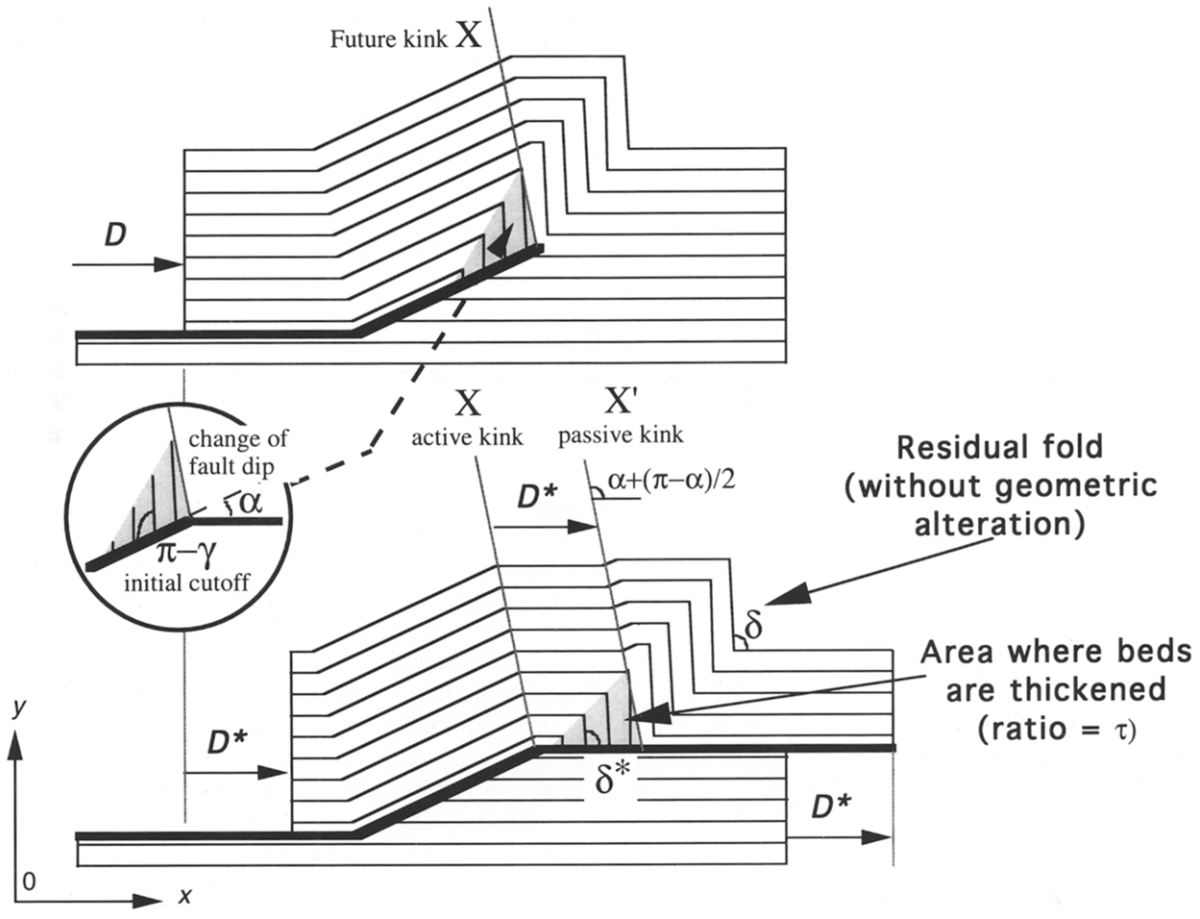

δ* = altered forelimb characteristic dip angle

D* = non-accommodated displacement

Fig. 5. Model of fault-propagation fold transported on the flat showing the parameters used in equations (10) and (11).

consequence of the requirement that the altered portion of the forelimb remains constant in area, the original forelimb beds situated between kinks X and X′ will have a smaller characteristic dip angle (δ^*) and will be thicker than the forelimb beds of the residual fold. The altered forelimb dip (δ^*) and altered thickness (e_f), expressed as percentage change (τ), are given by (modified from Mercier, 1992) as:

$$\delta^* = \arctan\left(\frac{1}{\frac{1}{\tan(\gamma)} - 2\tan(\alpha/2)}\right), \qquad (10)$$

$$\tau = 100\frac{e_f - e_i}{e_i} = 100\left(1 - \frac{\sin(\gamma)}{\sin(\delta^*)}\right). \qquad (11)$$

Note that by combining equations (4b) and (10), and equations (4b), (10) and (11) we could simply obtain the relationships between δ^* and α, and τ and α, respectively. These relationships are shown in Fig. 6. We emphasize that this geometric analysis is viable only if the dip of the forelimb is less than the dip of the kink fixed at the top of the ramp (Fig. 5). This assumption requires that the ramp angle be less than 30°, which is the upper limit of our model.

Figure 6 shows that the difference between δ and δ^* is generally insignificant. Consequently, and in contrast to Jamison's suggestion (1987), expressed again by Mitra (1990) and Anderson (1996) for example, the portion of FPF that moves through the upper ramp hinge will be geometrically different from a mode II fault-bend fold with the same ramp angle (Fig. 7).

The assumptions about the dip of the hinge fixed at the top of the ramp combined with the previous model (simple-step FPF), permit the equating of pre-'transport on the flat' intersections between the inter-beds and the kink-planes. Additionally, the input parameter 'non-accommodated slip' (D^*) permits derivation of these pre-transport locations to post-transport locations modelling a transport parallel to the thrust (Fig. 5).

Breakthrough fault-propagation folds

The breakthrough process occurs when the ramp propagation halts and a new fault segment develops,

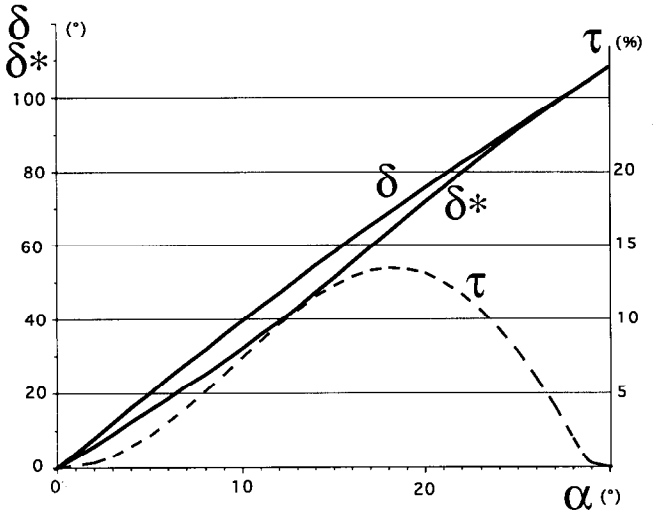

Fig. 6. Graph of ramp angle (α) versus forelimb dip (δ) in the residual fold, and forelimb dip (δ^*) and the thickness ratio (τ) in the altered forelimb according to equations (1), (4b), (10) and (11).

cutting through the fold. As a consequence of the slip on the new fault segment, a characteristic and distinctive fault-bend fold is produced and the FPF is altered by the thrust cutting through the fold (Suppe and Medwedeff, 1990) (Fig. 2). In our model, in accord with natural examples, the breakthrough thrust fault always cuts the forelimb of the fold. This corresponds to the classical concept of 'forelimb thrusts' (Dahlstrom, 1970; Butler, 1982). This implies that the thrust fault branches off from a place on the ramp between the synclinal and the anticlinal axial surfaces, including the limiting case where the thrust branches at the ramp tip and follows the synclinal axial surface (synclinal breakthrough) (Figs 2 & 8).

Geometrical analysis and modelling follow very similar lines to those described above for transport on the flat, but three new input parameters must be introduced: the value of non-accommodated slip (D^*), the location where the new fault branches off, and the dip of this new fault (ϕ).

As slip on the new fault segment takes place, in a manner analogous to transport on the flat, the axial plane of the new fold is fixed at the point of intersection of the new fault segment and the ramp. Moreover, the new fault cuts forelimb strata and individual hangingwall cut-off points and hinge points can be computed and modelled as previously. The parts of the fold that were already located ahead of the new active hinge (X) are transported, without alteration (Fig. 8). As in the case of transport on the flat, the part of the backlimb that is transported through the active synclinal hinge undergoes a bending parallel to the fault, and only the portion of the forelimb that is transported through this active hinge (grey area in Fig. 8) undergoes geometric alteration.

As the active hinge is synclinal, the problem of geometric alteration is very different to that explained for transport on the flat. The initial cut-off ($\pi - \gamma$) and change of fault dip (α) are the same, but Suppe (1983, fig. 7) has shown that a solution exists of parallel folding for such a situation. In other words, the beds of the forelimb portion transported through this active hinge (X), could undergo parallel folding. However, as illustrated and discussed in Mercier and Mansy (1995), a few natural examples of forelimbs transported through active synclinal hinges undergo shearing and thinning in agreement with the theoretical prediction of the 'bissectrix theory' (Mercier and Mansy, 1995). Thus, as for transport on the flat, we assume here that the kink fixed at the intersection of the ramp and the new fault bisects the angle between the two faults. As a consequence of the requirement that the altered portion of the forelimb remains constant in area, the beds in this portion will have a greater characteristic dip angle (δ^*) and be thinner than elsewhere (Fig. 8).

The altered forelimb dip (δ^*) and altered thickness (e_f), again expressed as a ratio, are given by:

$$\delta^* = \phi + \arctan\left(\frac{\sin(\gamma)\cos\left(\frac{\phi-\alpha}{2}\right)}{2\cos\left(\gamma-\frac{\phi-\alpha}{2}\right)-\cos(\gamma)\cos\left(\frac{\phi-\alpha}{2}\right)}\right), \quad (12)$$

$$\tau = 100\frac{e_f - e_i}{e_f} = 100\left(\frac{\sin(\delta^* - \phi)}{\sin(\gamma)} - 1\right). \quad (13)$$

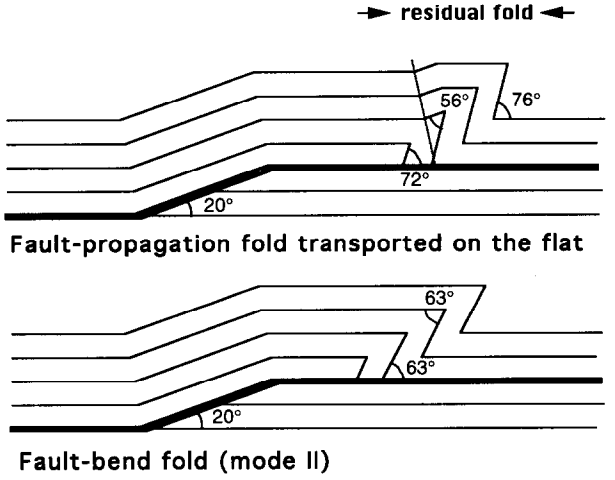

Fig. 7. Sketch showing that the altered portion of a fault-propagation fold is quite different from a fault-bend fold mode II (with the same ramp angle).

Note that by combining equations (4b) and (12), and equations (4b), (12) and (13) we obtain relationships between δ^* and α, and τ and α, respectively. These are graphed in Fig. 9.

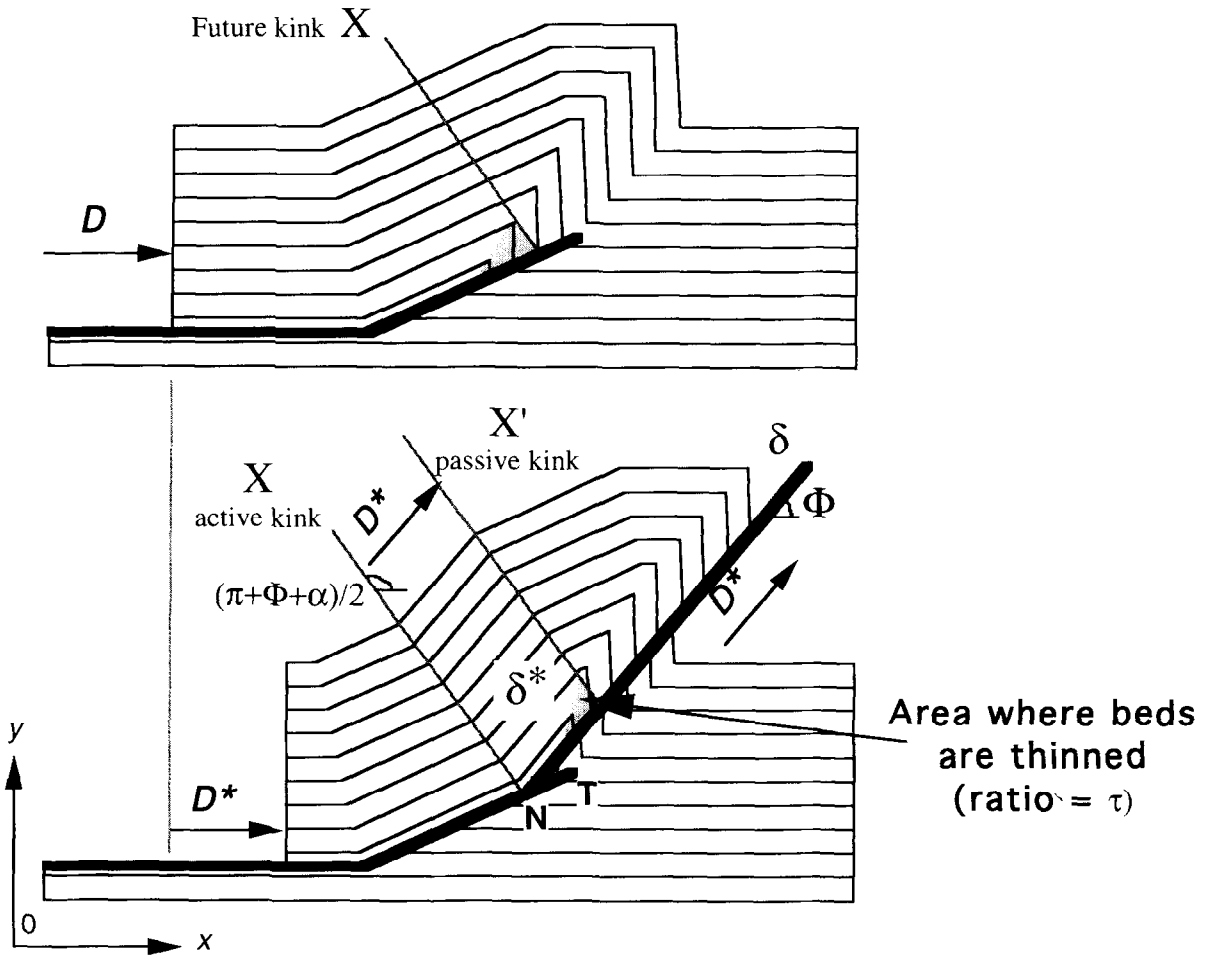

δ* = altered forelimb characteristic dip angle

D* = non-accommodated displacement

Φ = new fault angle

N = location of the new fault base (xN,yN); the value [NT] is a input parameter of our model

Fig. 8. Model of a fault-propagation fold in which the forelimb is cut by a breakthrough thrust showing the parameters used in equations (12) and (13).

APPLICATION TO A NATURAL EXAMPLE

Assumptions and use of the model

From a general point of view, our models follow the 'Suppe method' (Suppe, 1983) for drawing balanced cross-sections. This means that an application will be reliable only if the positions of some points are controlled. First, the folding style must be kink-like. Second, stratal thicknesses and lengths must remain constant through fold growth. We have seen, however, that, motived by theoretical considerations and/or natural examples, the models relax the classical constraint of constant thickness in very small zones situated in the forelimb, and involve thickening (Fig. 5) or thinning (Fig. 8) of beds as a consequence of late-stage evolution in this zone. Note that the constraint of constant area is never relaxed.

Additionally, our model assumes that deformation is completely accommodated by flexural slip (or flexural flow into the very small zones that undergo thickening or thinning) within the anticlines or, in other words, that no backshear or foreshear may be transmitted from the anticlines to the adjacent synclines. This point, that is often not taken into account in other models (Jamison, 1987; Endignoux and Mugnier, 1990; Mosar and Suppe, 1992; Mitra, 1992; Zoetemeijer and Sassi, 1992), seems to us particularly justified in thrust systems where, as in the example illustrated below, the synclines are very wide in comparison with the anticlines (see Martin and Mercier, 1994).

The balancing procedure allows the construction of successive geometries that are designated to simulate the natural tectonic process. The model is applied as follows: for each structure, the fault trajectory and the associated folding are defined *a priori*. The displacements are

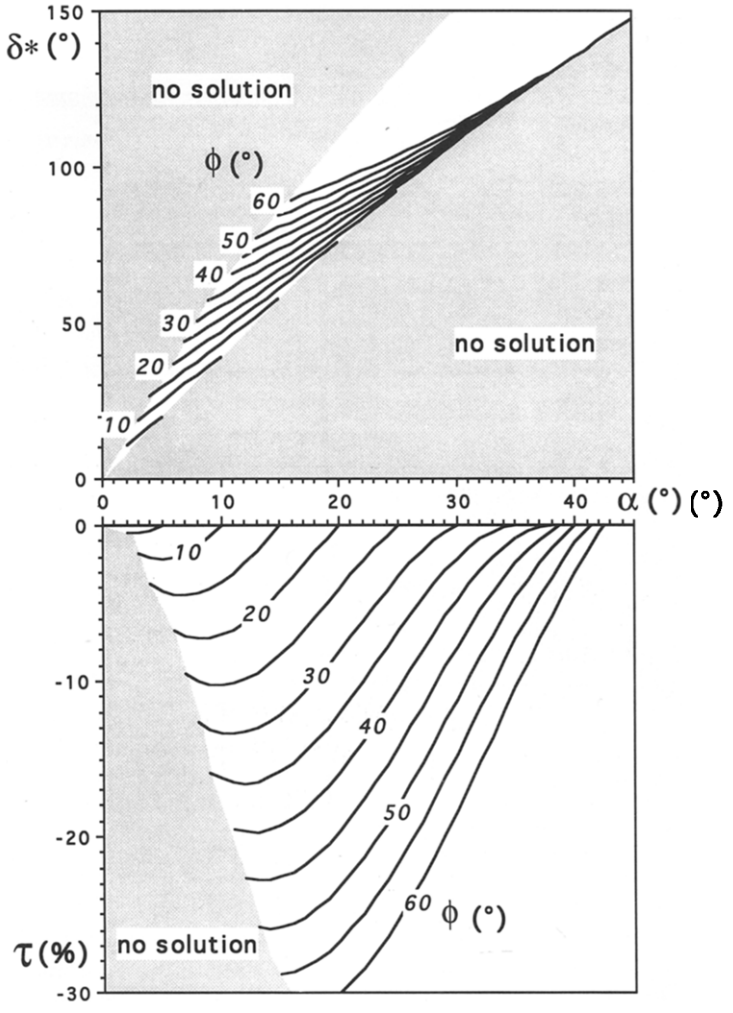

Fig. 9. Graphs of ramp angle (α) versus forelimb dips (δ^*) and the thickness ratio (τ) in the altered forelimb transported on a breakthrough thrust (dip = Φ, up to 60°) according to the equations (1), (4b), (12) and (13). The dotted area indicates the lack of solution (new fault dip > forelimb dip or < ramp dip).

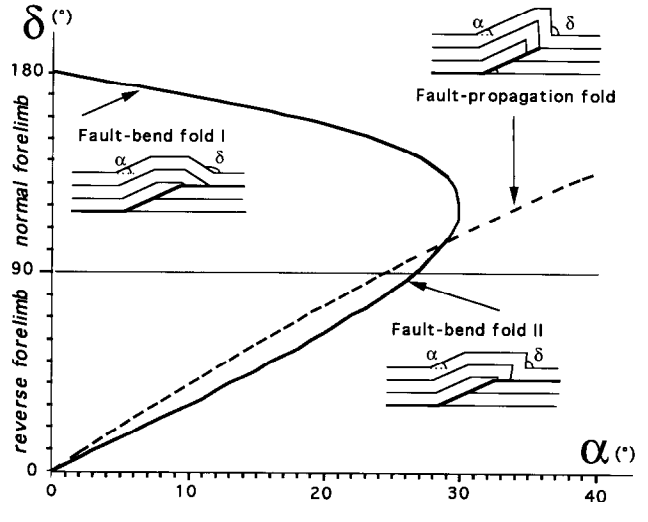

Fig. 10. Graphs of ramp angle (α) versus forelimb dip (δ) for different kinds of fault-related folds. These curves predict that there is no possible confusion of a fault-bend fold (mode I) with a fault-propagation fold (except if α is very close to 30°).

subsequently input and the geometry of the intermediate stages calculated successively. A trial and error method allows the constructed geometry to be fitted to the field data as explained below.

Natural example

Geometric analyses of one set of thrust-related folds from the Atlas Mountains of North Africa (Outtani *et al.*, 1995) near the orogenic front at the vicinity of the Algeria–Tunisia boundary, illustrate the use and some limitations of the model. In this region, many kilometric scale, asymmetric fault-related folds are exposed and the elevation of a particular stratigraphic unit, (if it is not involved in the thrust related structures) is quite constant. The E–W trending folds are generally developed in the Mesozoic–Cenozoic cover and are characterised by steep or overturned forelimbs. The lithologic succession consists mainly of carbonate and sandstone with occurrence of shale and evaporites that provide potential décollement levels. Tectonic transport is from north to south.

Identification of fault-propagation folds

If we consider, following many authors (Suppe, 1983; Jamison, 1987; Endignoux and Mugnier, 1990) that the fault-bend fold model II (Fig. 1) is likely a theoretical concept without geological meaning, asymmetric fault-related folds, characterized by steep or overturned forelimbs, call to mind a FPF process. However, as explained by Marshak and Woodward (1988) and Mitra and Namson (1989), some natural folds, that exhibit forelimb dips of around 70°–80° and backlimb dips (and consequently ramp dips) of around 30° (see Fig. 10), could be interpreted as fault-bend folds (mode I) as well as FPF. The curves of Fig. 10 show that the dips of backlimb (α) and forelimb ($\pi - \alpha$) vary in the same direction for fault-bend folds and in opposite directions for FPF. In the field, a fold never holds exactly the same geometry along strike, and both backlimb dip and forelimb dip change. Depending on the nature of the backlimb dip and forelimb dip variations (in the same direction or in opposite directions), the studied fold can be identified as a fault-bend fold or a fault-propagation fold (Fig. 10).

Use of the program

The selected cross-section (Fig. 11) includes a pair of E–W trending kink-folds, well exposed near the Atlas front. The geometrical pattern of the folds (kink-like, with overturned forelimb and residual fold) suggests that the Kebouda and Safit el Ouk folds are, respectively, a breakthrough FPF and a transported-on-the-flat FPF. First, the trial and error method allows us to model a geometry fitting the field data (dips and heights of the surface structure and offset of the merging fault) for the frontal fold behind the pin point. The trial and error method used to fit the model to the data is basically the

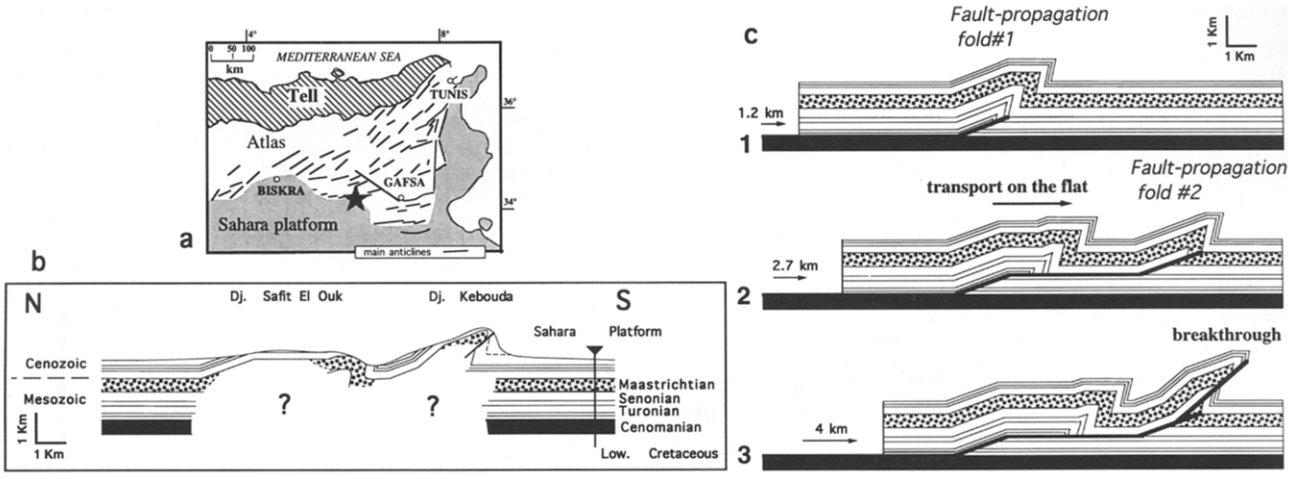

Fig. 11. Location (a), surface and subsurface data (b), and kinematic evolution of the studied natural example (c).

same as the one used to balance cross-sections by hand and to construct a deformed and restored section. The parameters fixed by the trial and error method are (see the Appendix): depth to décollement (1); location, height and dip of the ramp (2, 3, 4); location and dip of the breakthrough thrust fault (5, 6); and lastly, non-accommodated slip (7). Note that the identification as an FPF simplifies the balancing problem because the modelling of this kind of fold fixes both depth of the décollement and slip along the décollement level (contrary to a fault-bend fold, Mitra and Namson, 1989; Endignoux and Mugnier, 1990). In some cases, the occurrence of a single FPF in a complex cross-section can fix the depth to detachment of the whole section (Outtani *et al.*, 1995).

The modelling provides constraints on the geometry of the ramp, depth to décollement and slip values along this level (the slip accommodated in the fold is 1.5 km and non-accommodated slip is 1.3 km) (Fig. 11). These results have been used as input parameters in modelling of the rear fold. The value of slip behind the frontal fold (2.8 km) must be equal to the slip transmitted on the flat from the rear fold, and this flat must be at the same depth as the décollement beneath the frontal fold. In fact, the parameters fixed by the trial and error method are: depth to décollement (1); location, height and dip of the ramp (2, 3, 4). The depth of the upper décollement (5) and the amount of non-accommodated slip (6), two other input parameters, are fixed in the studied case. This provides accurate constraints for modelling the rear fold and fixing the geometry of the ramp (the depth to décollement) and the complete amount of slip.

The kinematic evolution (Fig. 11) deduced from the modelling is consistent with a forward translation (i.e. the amount of displacement on the flat) transmitted from the rear fold to the frontal fold. The latter acts as a fault-propagation fold which is cut out by a breakthrough thrust at a late stage. We emphasise that the building of these successive anticlines is done using only the standard fault-propagation folding mode and the late-stage evolution discussed in this paper.

CONCLUSIONS

Compared to other computer-aided models (Endignoux and Mugnier, 1990; Contreras and Sutter, 1990; Contreras, 1991; Zoetemeijer and Sassi, 1992), our approach mainly provides a balancing guideline for individual folds. Because it considers a wider variety of folding modes (and late stage alterations), its application to regional reconstruction clarifies the basic assumptions and enhances the reliability of balanced cross-sections.

We wish to emphasise the following points concerning fault-propagation folding: FPF does not always require the complete accommodation of the deformation within the fold, but can transfer slip toward the front of the structure (transport on the flat process); consequently the stair-case geometry of thrust faults is not necessarily indicative of fault-bend folding and FPF can be the main (and perhaps only) fault-related folding process in large areas of some thrust systems.

Acknowledgements—We wish to thank Dr P. Hudleston and an anonymous reviewer for significant improvements to our initial paper. This paper is a contribution to the Peri-Tethys programme.

REFERENCES

Alonso, J. L. and Teixell, A. (1992) Forelimb deformation in some natural examples of fault-propagation folds. In *Trust Tectonics*, ed. K. R. McClay, pp. 175–180. Chapman and Hall.

Anderson (1996) The Neogene structural evolution of the western margin of the Pelagian Platform, central Tunisia. *Journal of Structural Geology* **18**, 819–835.

Butler, R. W. H. (1982) The terminology of structures in thrust belts. *Journal of Structural Geology* **4**, 239–245.

Chester, J. S. and Chester, F. M. (1990) Fault-propagation folds above thrusts with constant dip. *Journal of Structural Geology* **12**, 903–910.

Contreras, J. (1991) Kinematic modeling of cross-sectional deformation sequences by computer simulation: coding and implementation of the algorithm. *Computers and Geosciences* **17**, 1197–1217.

Contreras, J. and Sutter, M. (1990) Kinematic modeling of cross-sectional deformation sequences by computer simulation. *Journal of Geophysical Research* **95**, 913–929.

Creuzot, G., Mercier, E., Ouali, J. and Tricart, P. (1993) La tectogenèse

atlasique en Tunisie centrale: apport de la modélisation géométrique. *Eclogae geologica Helvetica* **86/2**, 609–627.

Dahlstrom, C. D. A. (1970) Structural geology in the eastern margin of the Canadian Rocky Mountains. *Bulletin of Canadian Petroleum Geology* **18**, 332–406.

Endignoux, L. and Mugnier, J. L. (1990) The use of a forward kinematical model in the construction of balanced cross-sections. *Tectonics* **9**, 1249–1262.

Jamison, W. R. (1987) Geometric analysis of fold development in overthrust terranes. *Journal of Structural Geology* **9**, 207–219.

Marshak, S. and Woodward, N. (1988) Introduction to cross-section balancing. *Basic Methods of Structural Geology*, eds S. Marshak and G. Mitra, pp. 303–332. Prentice Hall.

Martin, J. and Mercier, E. (1994) L'accommodation locale: une solution alternative au problème de la conjonction des plans de kinks dans l'équilibrage d'une coupe (exemple dans le Jura externe). *Comptes Rendus de l'Académie des Sciences, Paris* **318/II**, 1111–1115.

Martin, J. and Mercier, E. (1996) Héritage distensif et structuration chevauchante dans une chaîne de couverture Apport de l'équilibrage par modélisation géométrique dans le Jura nord-occidental. *Bulletin of geological Society France*. **167**, 101–111, erratum p. 194.

McClay, K. R. (1992) Glossary of thrust tectonics terms. In *Thrust Tectonics*, ed. K. R. McClay, pp. 419–433. Chapman and Hall.

Mercier, E. (1992) Une évolution possible des chevauchements associés aux plis de propagation: le transport sur le plat (modélisation et exemple). *Bulletin de la Société géologique de France* **163**, 713–720.

Mercier, E., De Putter, T., Mansy, J. L. and Herbosch, A. (1994) L'écaille des Gaux (Ardennes belges): un exemple d'évolution tectono–sédimentaire complexe lors du développement d'un pli de propagation. *Geologische Rundschau* **83**, 170–179.

Mercier, E., Outtani, F., Frizon de Lamotte, D. and Ghandriche, H. (1995) Geometry of fault-propagation folds: method and application — Comment. *Tectonophysics* **245**, 111–113.

Mercier, E. and Mansy, J. L. (1995) Le blocage du transport sur le plat des plis de propagation: une cause possible des chevauchements hors séquence. *Geodynamica Acta* **8**, 199–210.

Mitra, S. (1990) Fault-propagation folds: geometry, kinematic evolution and hydrocarbon traps. *American Association of Petroleum Geologists Bulletin* **74**, 921–945.

Mitra, S. (1992) Balanced structural interpretations in fold and thrust belts. In *Structural Geology of Fold and Thrust Belts*, eds S. Mitra and G. W. Fischer, pp. 53–77. Johns Hopkins Univ. Press, Baltimore.

Mitra, S. and Namson, J. (1989) Equal-area balancing. *American Journal of Science* **289**, 563–599.

Mosar, J. and Suppe, J. (1992) Role of shear in fault-propagation folding. In *Thrust Tectonics*, ed. K. R. McClay, pp. 123–132. Chapman and Hall.

Outtani, F., Addoum, B., Mercier, E., Frizon de Lamotte, D. and Andrieux, J. (1995) Geometry and kinematics of the South Atlas Front (Algeria–Tunisia). *Tectonophysics* **249**, 233–248.

Philippe, Y. (1994) Transfer zone in the southern Jura thrust belt (Eastern France): Geometry, development and comparison with analogue modelling experiments. In *Hydrocarbon and Petroleum Geology of France*, ed. A. Mascle, pp. 327–346. E.A.P.G. memoir.

Suppe, J. (1983) Geometry and kinematics of fault-bend folding. *American Journal of Science* **283**, 684–721.

Suppe, J. (1985) *Principles of Structural Geology*. Prenctice Hall.

Suppe, J. and Medwedeff, D. A. (1984) Fault-propagation folding. *G.S.A. abstracts with programs* **16**, 670.

Suppe, J. and Medwedeff, D. A. (1990) Geometry and kinematics of fault-propagation folding. *Eclogae geologica Helvetica* **83**, 409–454.

Thompson, R. I. (1981). The nature and significance of large blind thrusts within the northern Rocky Mountains of Canada. In *Thrust and Nappe Tectonics*, eds K. R. McClay and N. J. Price, Vol. 9, pp. 449–462. Special Publication of Geological Society London.

Zoetemeijer, R. and Sassi, W. (1992). 2-D reconstruction of thrust evolution using the fault-bend method. In *Thrust Tectonics*, ed. K. R. McClay, pp. 133–140. Chapman and Hall.

APPENDIX

The Rampe(EM) 2.1.x program

An interactive graphics software, Rampe(EM), was used to produce many figures of this paper. It is freely available from the first author. This program, compiled for the Macintosh computer, was developed using the above equations and procedures. It can also model fault-bend folds (modes I and II), using equations developed by Suppe 1983, 1985, and the folds of Chester and Chester (1990). The program uses the standard Macintosh interface using the mouse as the main input device. The program generates pictures of both sections before and after deformation and a table of numerical results. These output sheets can be printed or sent to the 'clipboard' in PICT format, so that pictures can be pasted into a drawing program in order to be completed and printed.

During a typical session, the program runs as follows. Rampe(EM) requires that at least one bed be drawn in the cross-section. The stratigraphic 'layer cake' could be input from the keyboard in pixels (and saved in a stratigraphic file) or imported from such a file previously created. Then, if the FPF module is selected, the following input parameters are required: (1) depth to décollement, (2) height and (3) dip of the ramp; and (4) the non-accommodated slip. If the last parameter is zero, three output sheets are generated. If this parameter is not zero, the user must select a kind of late-stage evolution. In the case of transport on the flat, the output sheets are again generated. In the case of breakthrough, the program calculates the possible locations of the base of the new fault so that the new fault remains within the forelimb. Then this location must be specified. Depending on the location, the program calculates the range of possible dips of the new fault. The dip must then be specified and the three output sheets are then generated.